Biochimica et Biophysica Acta, 1144 (1993) 325–330

BBABIO 43881

Stark effect spectroscopy of the 1250 nm P^+ band of *Rhodobacter sphaeroides* reaction centers and related model compounds

Jonathan W. Stocker, Stephan Hug and Steven G. Boxer

Department of Chemistry, Stanford University, Stanford, CA (USA)

(Received 19 January 1993)

Key words: Photosynthesis; Reaction center; Stark spectroscopy; Mixed valence

The absorption and Stark effect spectra of the 1250 nm band associated with the oxidized special pair (P^+) in *Rhodobacter sphaeroides* reaction centers have been measured. The absorption spectrum in the 1000–1450 nm region is essentially identical whether P^+ is generated by chemical oxidation or continuous illumination. The Stark effect on the 1250 nm band of P^+ is relatively small compared to the Stark effect seen for the Q_Y transition of P. A quantitative analysis indicates that the change in dipole moment for the 1250 nm band is very small. These results are compared with data for two model systems: a lanthanide-bridged porphyrin dimer, $Eu(OEP)_2$, and a mixed valence coordination complex, the Creutz-Taube ion. The Stark effect spectrum of the 1250 nm P^+ band is found to be similar to both of these systems. This contrasts with valence-trapped systems whose mixed valence transitions exhibit a large change in dipole moment (Oh, D. and Boxer, S.G. (1990) J. Am. Chem. Soc. 112, 816; Oh, D. and Boxer, S.G. (1991) J. Am. Chem. Soc. 113, 6880). These results, together with other observations on the spectrum of reaction centers in the P^+ state, are consistent with the view that the 1250 nm electronic transition of P^+ is delocalized over the two bacteriochlorophyll molecules comprising the special pair.

Introduction

The characteristic EPR and endor properties of the cation radical produced in the initial photoinduced electron-transfer step of photosynthesis have been essential for establishing whether the primary electron donor, P, is a monomer or dimer [1–3]. In the case of bacterial reaction centers (RCs), the EPR linewidth of P^+ is narrower than for the cation radical of an isolated monomeric bacteriochlorophyll (BChl) [1,2]. In combination with endor data, these observations led to the early suggestion that P is a dimer of BChls [1,4]. The three-dimensional structure of the RC confirms that two BChls are in close proximity in the primary electron donor [5,6]. Detailed characterization of the unpaired spin density distribution in P^+ by endor continues to be a rich area of investigation (see, e.g., Ref. 7).

While EPR and endor are exquisitely sensitive to the unpaired spin density distribution in P^+, they are intrinsically limited to probing this information quite long after P^+ is formed (typically fractions of μs or longer). Because the initial charge separation step occurs in a few ps, the nature of P^+ as it is initially formed is an important issue. It has been known for many years that P^+ also has a characteristic electronic absorption band in the near infra-red at about 1250 nm [8,9], and this absorption feature has been used on occasion to monitor the short-time kinetics of the RC [10,11]. In contrast to the ground state absorption of P, which has been discussed at great length in the literature, the 1250 nm P^+ has not been the subject of as much interest. Very recently, another low-lying electronic transition of P^+ has been discovered at 2600 cm^{-1} in the mid-infrared [12]. This band, likewise, is sensitive to the electronic coupling and delocalization in P^+. Because both the 1250 nm and 2600 cm^{-1} bands can be detected with whatever time resolution is available, it is useful to understand the electronic origin of these bands.

In the following, we report the Stark effect on the absorption spectrum of the 1250 nm band and compare the results to related experiments on the ground state of P [13–16], some transition metal mixed-valence complexes [17,18], and a lanthanide-bridged porphyrin (octaethylporphyrin, OEP) dimer, $Eu(OEP)_2$, which is a synthetic model for P^+ [19]. From the viewpoint of a Stark effect experiment, very different results are expected depending on whether the electronic state is localized or delocalized. For a localized (valence-

Correspondence to: S.G. Boxer, Department of Chemistry, Stanford University, Stanford, CA 94305-5080, USA.

trapped) mixed-valence system, such as M^{2+}-L-M^{3+}, where M^{+n} is a metal ion and L is a bridging ligand, a substantial ground-state dipole is present, and photoexcitation of the mixed-valence transition reverses the direction of this dipole (M^{2+}-L-$M^{3+} \rightarrow M^{3+}$-L-$M^{2+}$) . The ground and excited-state dipole moments are antiparallel to each other, and a large change in dipole moment, $|\Delta\mu|$, is expected. In the other limit, if the hole is delocalized, then no change in dipole moment is expected. At a qualitative level, when a change in dipole moment dominates, the lineshape of the Stark effect spectrum for an isotropic, immobilized sample, is approximated by the second derivative of the absorption lineshape [20]. If the change in dipole moment is small, then other effects such as the change in polarizability, and transition polarizability and hyperpolarizability lead to Stark effect lineshapes which resemble combinations of zeroth and first derivatives of the absorption spectrum. To the extent that the 1250 nm P^+ transition can be viewed as related to a mixed-valence transition (see below), even at a qualitative level, the Stark effect spectrum can provide a sensitive probe of the degree of delocalization of the 1250 nm transition.

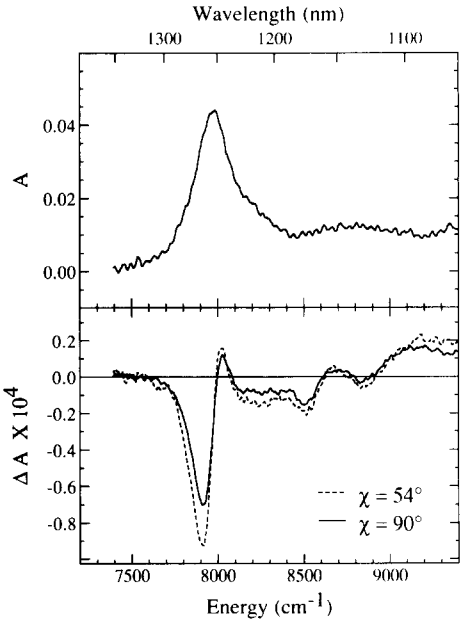

Fig. 2. (A) P^+ absorption spectrum produced by chemical oxidation of reaction centers with $K_3[Fe(CN)_6]$ (glycerol/buffer glass at 77 K in a 100 μm pathlength cell). (B) Stark effect spectrum of the same sample as panel A (applied external field $2.4 \cdot 10^5$ V/cm).

Materials and Methods

Photosynthetic RCs were isolated from *Rb. sphaeroides*, R26, by standard methods [21]. P^+ can be generated either by chemical oxidation with $K_3Fe(CN)_6$ or by photoexcitation. Stark effect spectra were obtained on chemically oxidized samples, while absorption lineshapes, used to obtain the derivatives needed for data analysis, were obtained by both methods. The equivalence of these two methods of preparation is discussed below. The extinction coefficient of the 1250 nm band is quite small (ε approx. 20 cm^{-1} mM^{-1}), and the Stark spectra must be obtained on thin samples (thickness approx. 100 μm), therefore, concentrated RC solutions were chemically oxidized for the Stark measurements. In a typical experiment, samples which were 10–100 μM in RCs were oxidized by excess potassium ferricyanide (typically 40–50 mM) in a solvent consisting of 50% glycerol/50% buffer (10 mM Tris (pH 8.0), 0.05% LDAO buffer). The samples were immediately introduced into the sample cell and plunged into liquid nitrogen.

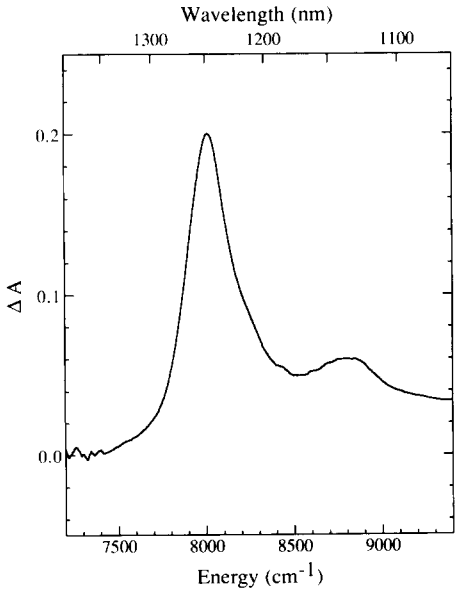

Fig. 1. Light-induced absorption spectrum of *Rb. sphaeroides* reaction centers in the 7200 cm^{-1}–9500 cm^{-1} region showing the P^+ absorption band (glycerol/buffer glass at 77 K in a 500 μm pathlength cell).

Stark effect spectra were obtained using methods described elsewhere for frozen glycerol/buffer glasses [20,22,23]. These experiments provide an excellent example of one of the advantages of using frozen samples rather than polymer films for obtaining Stark effect data [20]. The detector was a Ge-photodiode for the 900–1500 nm region (Judson IR, Model J16). The light-minus-dark difference spectra were obtained by exciting an RC sample (500 μm thick sample cell filled with 100 μM RCs in glycerol/buffer solution) with light from an Ar-ion laser (all lines). The sample transmission was probed with light from a 100 W tungsten-halogen lamp passed through a monochromator and was chopped at 400 Hz before impinging on the sample. It is rather difficult to obtain an accurate baseline

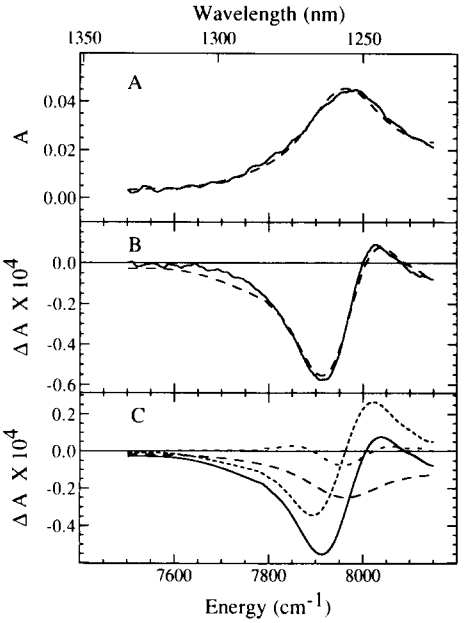

Fig. 3. (A) Absorption spectrum (———) and fit (------) of chemically-oxidized reaction centers between 7500 cm^{-1} and 8150 cm^{-1} (same sample as Fig. 2, 77 K). (B) Stark effect spectrum (———) and fit (------) of same sample as in panel A. (C) Fit (———) to the Stark effect spectrum composed of zeroth (— — —), first (------) and second (· · · · · ·) derivative components of absorption obtained from the simultaneous best fit of both the absorption and Stark spectra.

for the 1250 nm band, both because there is broad underlying absorption and because the absorption is so weak. This causes some uncertainty in the quantitative analysis of the Stark effect spectra since this requires accurate first and second derivatives of the absorption (see below). The absorption and Stark effect (ΔA) have been set equal to zero at energies below 7500 cm^{-1} which is well below the energy of any major feature in the spectra.

$Eu(OEP)_2$ was obtained as a generous gift from Prof. David Bocian or it was prepared as described in Refs. 24 and 25. Stark spectra were obtained on polystyrene films (average molecular mass 430 kDa) as described for other organic chromophores [13,14].

Results

The light-minus-dark difference spectrum of RCs in the 1060 to 1350 cm^{-1} region is shown in Fig. 1. The main feature of the spectrum is an absorption band centered at 1250 nm. A smaller band centered around 1125 nm is also observed, along with a small increase in absorption in the entire wavelength region between the bleach of the special pair Q_Y band centered at 870 nm and the band at 1250 nm, with some structure in the region between 920 nm and 1020 nm (results not shown) [1]. The larger band has its maximum at 1250 nm with a full-width-at-half-maximum of 280 ± 20 cm^{-1}. Because of the assumed one-to-one correlation between the bleach of the 870 nm hand and the appearance of the 1250 nm band, a comparison of the relative amplitudes of these two features can be used to estimate the extinction coefficient of the 1250 nm band, giving 20 $cm^{-1}\,mM^{-1}$ based on the 870 nm band (114 $cm^{-1}\,mM^{-1}$).

Fig. 2A shows the absorption in the 1060–1350 nm region following chemical oxidation of RCs with potassium ferricyanide. The 1250 nm band is essentially identical to the band generated by photoexcitation (cf., Fig. 1). The Stark effect spectrum of the identical sample is shown in Fig. 2B. Fig. 3 shows an expanded view of the absorption, Stark effect, and a best fit to a sum of derivatives of the absorption and is discussed below.

The near infrared absorption band of $Eu(OEP)_2$ at 77 K is shown in Fig. 4A. Fig. 4B shows the Stark effect and a fit to that band. The fit was accomplished by using the zeroth, first, and second derivative components of a fit to the absorption, and the components are shown in Fig. 4C.

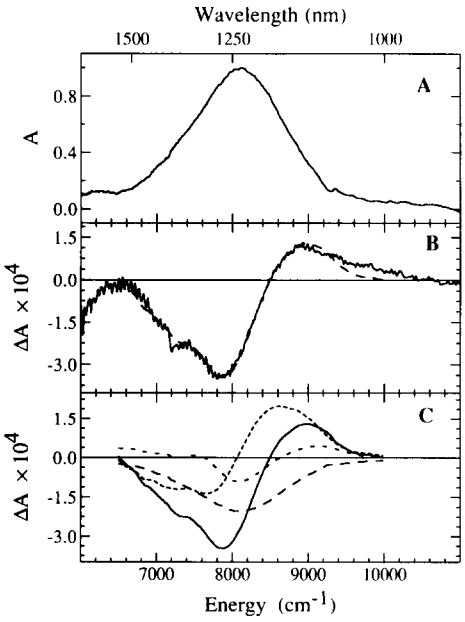

Fig. 4. (A) Absorption (scaled to $A = 1$ at the absorption maximum) and (B) Stark effect spectrum of $Eu(OEP)_2$ in polystyrene at 77 K (ΔA scaled to its value at $1.0 \cdot 10^6$ V/cm). (C) Fit (———) to the Stark effect spectrum composed of zeroth (— — —), first (------) and second (· · · · · ·) derivative components of absorption.

[1] It is of interest to note that similar small absorption features are apparent in all RC mutants which have been looked at by this lab using this method. This includes mutants such as the *Rb. sphaeroides* heterodimer ((M)H202L) which has no apparent 1250 nm band under similar conditions (unpublished results).

Discussion

Absorption of P^+ and $Eu(OEP)_2$

The 1250 nm absorption band is unique to the cation radical of the dimeric special pair. It is not observed upon chemical oxidation of monomeric BChl in vitro [8]. Although this transition has been used as an optical fingerprint for P^+, the nature of this electronic transition has not been extensively discussed. The absorption spectrum has several noteworthy properties. (i) Within the signal-to-noise, the 1250 nm band is identical whether P^+ is generated by chemical oxidation or photochemically. (ii) The linewidth of the 1250 nm band (280 cm^{-1}) is considerably smaller than that of the Q_Y transition of the unoxidized special pair (about 520 cm^{-1}) under identical conditions. (iii) Additional structure is observed at higher energy, notably the band at 1125 nm (a shift of about 880 cm^{-1} from the 1250 nm band). It is quite possible that the weaker band seen at 1125 nm is part of a vibronic progression [2].

A similar near-infrared band is seen in some lanthanide octaethylporphyrin sandwich complexes such as $Eu(OEP)_2$ (Fig. 4A) [19]. This complex contains a hole in the porphyrin π-system and can be viewed as a model for P^+. Under conditions reported in this paper the near-infrared absorption band of $Eu(OEP)_2$ has a width which is at least a factor of five greater than that of the 1250 nm band of P^+. At low temperatures in deuterated solvents, Duchowski and Bocian have reported resolved structure in the near-infrared band of $Eu(OEP)_2$ [19]. We were unable to reproduce this structure for samples provided by Prof. Bocian (same samples as those used in Ref. 19) or for those prepared in our laboratory; however, the band around 1250 nm, which is characteristic of the correct oxidation state, is present in our samples. The linewidth is reported to be sensitive to solvent and sample preparation which may explain the absence of structure in our spectra. Interestingly, the individual features within the well-resolved vibronic progression reported by Duchowski and Bocian [19] have linewidths on the order of 200 cm^{-1}. Simulation of the observed spectra was accomplished using two origins separated by 400 cm^{-1}, with vibronic progressions of approx. 250 cm^{-1} and approx. 310 cm^{-1}. It was suggested that the two origins arise from two distinct conformers of the dimer, and the structure is due to a vibrational mode which modulates the inter-ring distance. It is possible that the band at 1125 cm^{-1} in the P^+ spectrum is also due to a vibronic progression, though likely with a different physical origin.

Shark effect spectra of P^+, $Eu(OEP)_2$ and the mixed-valence system

It is immediately apparent that there is little change in dipole moment associated with the 1250 nm transition of P^+, as there is no evidence for a significant second derivative contribution to the Stark effect lineshape. This result is independent of the precise choice of baseline for absorption or ΔA. It is in striking contrast with the electronic ground state of P, whose Stark effect spectrum is dominated by a second derivative contribution [13,15,16].

The Stark effect spectrum can be analyzed more quantitatively by comparing $\Delta A(\nu)$ with the derivatives of the absorption. When an external electric field is applied to a non-oriented and immobilized sample, the change in absorption can be modelled as:

$$\Delta A(\nu) = (f\mathbf{F}_{ext})^2 \left\{ A_\chi A(\nu) + \frac{B_\chi}{15hc} \frac{\nu \, d[A(\nu)/\nu]}{d\nu} + \frac{C_\chi}{30h^2c^2} \frac{\nu \, d^2[A(\nu)/\nu]}{d\nu^2} \right\} \quad (1)$$

where ν is energy in wavenumbers, h is Planck's constant and c is the speed of light [20]. The local field correction factor f relates the magnitude of the field present at the chromophore, $\mathbf{F}_{int}$, to that of the externally applied field: $\mathbf{F}_{int} = f \cdot \mathbf{F}_{ext}$. [3] χ is the angle between the applied electric field direction and the polarization vector of the probe beam. The coefficients A_χ, B_χ and C_χ depend on a variety of molecular parameters. The second derivative component, C_χ, is associated exclusively with a change in the permanent dipole moment. The first derivative contribution, B_χ is due to changes in polarizability between the ground and excited states, though contributions from the cross-term between the transition moment polarizability and difference dipole moment can contribute. The zeroth derivative component, A_χ, is due to changes in the polarizability and/or hyperpolarizability of the transition moment.

The simplest approach to the analysis of Stark effect spectra is to decompose the Stark effect signal, ΔA, into a sum of contributions from the three derivatives of A. We have shown recently that this overempha-

[2] In principle, the 1125 nm feature could be the upper exciton band associated with the 1250 nm transition. This is unlikely as the exciton splitting should scale as the square of the transition dipole strength. The latter is much smaller for the 1250 nm P^+ absorption than for the Q_Y transition of BChl.

[3] In this paper, we are primarily concerned with the contributions to the Stark effect lineshapes. The value of f appears as a common multiplier of each derivative term in Eqn. 1, so its value does not enter differentially into the decomposition of ΔA. When values are given for $|\Delta\boldsymbol{\mu}|$ and for $|Tr\Delta\boldsymbol{\alpha}|$, the numerical values are given in terms of f as Debye/f and $Å^3/f^2$, respectively.

sizes the absorption spectrum in the analysis [16]. Although the absorption spectrum often has low noise, its derivatives do not. The quality of ΔA is often very high, and, as in the present case, the absorption is weak. Therefore, we have implemented an approach based on simultaneously fitting A and ΔA, thereby giving comparable weight to both as is appropriate to the experimental uncertainties. The dashed lines in Fig. 3A and B show the best simultaneous fit of both the absorption and Stark effect bands of P^+ using this strategy. Considering the signal-to-noise, limited by the small extinction coefficient and the detector sensitivity, the fit of both spectra is reasonably good. Fig. 3C shows the zeroth, first, and second derivative components which are summed to give the overall best fit shown in Fig. 3B. As expected by qualitative inspection, there is only a very small second derivative component to the fit, demonstrating that $|\Delta\mu|$ is very small (< 1.0 Debye$/f$). This small contribution argues strongly against a significant change in the electron distribution between the ground and excited states of P^+ for this transition. The counterion for P^+ is either Q^-_A, when P^+ is formed by photoexcitation, or it is the Fe(II) ion somewhere in solution. In either case, a well-defined dipole moment exists both in the ground and excited state of P^+, and the position of the counterion does not move at the instant P^+ is excited. If the hole on P^+ were localized on one macrocycle in the ground state and moved to the other upon photoexcitation at 1250 nm, we would expect a change in dipole moment, $\Delta\mu$, irrespective of the location of the counterion. The Stark effect data indicate that $|\Delta\mu|$ is very small for the 1250 nm band, and this is consistent with a small change displacement of charge associated with photoexcitation of P^+. Recent theoretical analysis of the 1250 nm band likewise suggests that $|\Delta\mu|$ should be small for this transition (Parson, W.W., personal communication).

The dominant contribution to ΔA for the 1250 nm band is from a negative first derivative of the absorption. As discussed above, the zeroth and first derivative contributions contain a number of terms which can cancel and are much more difficult to interpret in terms of optoelectronic factors. The amplitude of the first derivative contribution to the 1250 nm P^+ band is considerably smaller than for the Q_Y band of P, and the sign is reversed [16]. We have argued elsewhere that mixing with a charge-transfer state (s) should and does lead to a substantial excited state polarizability for *P [16]; this does not appear to be significant for the 1250 nm transition. Assuming that the entire first derivative component is due to a change in polarizability (i.e., there is no contribution from the polarizability of the transition moment), we obtain $|Tr(\Delta\alpha)|$ approx. -100 Å$^3/f^2$, compared to $|Tr(\Delta\alpha)|$ approx. 900 Å$^3/f^2$ for P [16]. The size of the zeroth derivative contribution is small, which is consistent with the expectation that the contribution of the polarizability of the transition dipole moment is small. Note also that any contributions from the hyperpolarizability of the transition dipole moment is not considered in this analysis. The simplest explanation for the lineshape is that there is a decrease in polarizability upon excitation at 1250 nm. This is not without precedent [18], though it is quite unusual.

The near infrared feature of $Eu(OEP)_2$ in Fig. 4, which has its maximum at 1250 nm, is similar to that seen for the 1250 nm band of P^+, except that the linewidth in our spectrum is about a factor of 5-times larger than the 1250 nm band of P^+. As discussed above, the apparent width of the 1250 nm band for $Eu(OEP)_2$ is sensitive to inhomogeneous broadening, and the underlying features have been shown to have linewidths comparable to those of P^+ [19]. In spite of this difference in inhomogeneous linewidths, the lineshapes of the Stark spectra of the 1250 nm bands in $Eu(OEP)_2$ and P^+ are qualitatively similar (compare Figs. 3B and 4B). The Stark effect spectrum of $Eu(OEP)_2$ shows a large negative first derivative component and a small, positive second derivative component with almost no zeroth derivative component. From

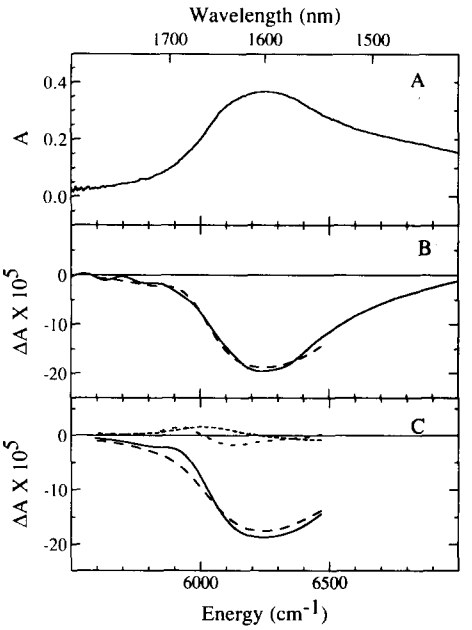

Fig. 5. (A) Absorption and (B) Stark effect spectrum (solid line) for the Creutz-Taube ion, $[NH_3)_5Ru(pyrazine)Ru(NH_3)_5]^{5+}$, in the mixed-valence region taken from Ref. 18 (50% glycerol/H_2O at 77 K and $\mathbf{F}_{ext} = 4 \cdot 10^5$ V/cm). The dashed line in (B) is the best fit to the Stark effect spectrum where only the region at lower energy than 6500 cm^{-1} is shown (other absorption features are present at higher energy). The decomposition of this fit is shown in (C) consisting of zeroth (— — —), first (------) and second (· · · · · ·) derivative components of the fit to the absorption spectrum and suming to the best-fit curve (———).

a quantitative analysis, $|\Delta\mu|$ is calculated to be about 1.0 Debye/f.

We have recently published an extensive analysis of the Stark effect spectra of classical mixed-valence systems of the general type Ru(II)-ligand-Ru(III). The degree of delocalization in this class of compounds has been the subject of enormous work, and the results are directly relevant to the data in this paper and to more general problems in electron transfer [26]. As an illustration, the absorption and Stark effect spectra of the mixed valence transition of the Creutz-Taube ion, Ru(II)-pyrazine-Ru(III) [27], are shown in Fig. 5 (data taken from Ref. 18). There is a striking qualitative resemblence between the ΔA spectra for the mixed valence transition and the 1250 nm P^+ band, especially the nearly complete absence of a second derivative ($|\Delta\mu|$) contribution. By contrast, valence-trapped systems, such as Ru(II)-4,4′-bipyridine-Ru(III), have Stark spectra which are completely dominated by contributions from the second derivative of the absorption [18]. This comparison reinforces the conclusion reached above that the 1250 nm P^+ transition does not involve a significant change in the localization of the hole between the ground and excited states. Experiments to measure $|\Delta\mu|$ for the recently discovered 2600 cm^{-1} band of P^+ [12] are in progress.

Acknowledgements

We are grateful to Professor Bocian who provided the original samples of $Eu(OEP)_2$ and for useful discussions. We also thank Dr. Kaiqin Lao and Martin Steffen for helpful discussion. Parts of this work were supported by grants from the National Science Foundation Chemistry and Biophysics Programs. J.W.S. was an NSF Pre-doctoral and Veatch Fellow; S.H. was a Fellow of the Swiss National Science Foundation.

References

1 Norris, J.R., Uphaus, R.A., Crespi, H.L. and Datz, J.J. (1971) Proc. Natl. Acad. Sci. USA 68, 625.
2 McElroy, J.D., Feher, G. and Mauzerall, D.C. (1972) Biochim. Biophys. Acta 267, 363.
3 Lendzian, F., Lubitz, W., Scheer, H., Bubenzer, C. and Mobius, K. (1981) J. Am. Chem. Soc. 103, 4635.
4 Feher, G., Hoff, A.J., Isaacson, R.A. and Ackerson, L.C.F. (1975) Ann. N.Y. Acad. Sci. 224, 239.
5 Deisenhofer, J., Epp, O., Miki, K., Huber, R. and Michel, H. (1984) J. Mol. Biol. 180, 385–398.
6 Deisenhofer, J., Epp, O., Miki, K., Huber, R. and Michel, H. (1985) Nature 318, 618.
7 Lendzian, F., Bönigk, B., Plato, M., Möbius, K. and Lubitz, W. (1992) in Structure, Function and Dynamics of the Bacterial Reaction Center, (Breton, J. and Vermeglio, A., eds.), Plenum Press, p. 89.
8 Fajer, J. Borg, D.C., Forman, A., Felton, R.H., Dolphin, D. and Vegh, L. (1974) Proc. Natl. Acad. Sci. USA 71, 994.
9 Fajer, J., Brune, D.C., Davis, M.S., Forman, A. and Spaulding, L.D. (1975) Proc. Natl. Acad. Sci. USA 72, 4956.
10 Dutton, P.L., Kaufmann, K.J., Chance, B. and Rentzepis, P.M. (1975) FEBS Lett. 60, 275.
11 Martin, J.-L., Breton, J., Hoff, A.J., Migus, A. and Antonetti, A. (1986) Proc. Natl. Acad. Sci. USA 83. 957.
12 Breton, J., Nabedryk, E. and Parson, W.W. (1992) Biochemistry 31, 7503.
13 Lockhart, D.J. and Boxer, S.G. (1987) Biochemistry 26, 664–668.
14 Lockhart, D.J. and Boxer, S.G. (1987) Proc. Natl. Acad. Sci. 85, 107–111.
15 Lösche, M. Feher, G. and Okamura, M.Y. (1987) Proc. Natl. Acad. Sci. USA 84, 7537,
16 Middendorf, T.R., Mazzola, L.T., Lao, K., Steffen, N.A. and Boxer, S.G. (1993) Biochim. Biophys. Acta 1143, 223–234.
17 Oh, D.H. and Boxer, S.G. (1990) J. Am. Chem. Soc. 112, 8161–8162.
18 Oh, D.H., Sano, M. and Boxer, S.G. (1991) J. Am. Chem. Soc. 113, 6880.
19 Duchowski, J.K. and Bocian, D.F. (1990) J. Am. Chem. Soc. 112, 3312.
20 Boxer, S.G. (1993) in Photosynthetic Reaction Centers (Norris, J. and Deisenhofer, J., eds.), Academic Press, Vol. 2, pp. 179–220.
21 Schenck, C.C., Blankenship, R.E. and Parson, W.W. (1982) Biochim. Biophys. Acta 680, 44–59.
22 Hammes, S., Mazzola, L., Boxer, S.G., Gaul, D. and Schenck, C. (1990) Proc. Natl. Acad. Sci. USA 87, 5682–5686.
23 Gottfried, D.S., Stocker, J.W. and Boxer, S.G. (1991) Biochim. Biophys. Acta 1059, 63–90.
24 Buchler, J.W., DeCian, A., Fischer, J., Kihn-Botulinski, M. and Weiss, R. (1988) Inorg. Chem. 27, 339.
25 Buchler, J.W. and Loffler, J. (1990) Z. Nat.forsch., Teil B 45, 531.
26 Hush, N.S. (1967) Prog. Inorg. Chem. 8, 391–444.
27 Creutz, C. and Taube, H. (1969) J. Am. Chem. Soc. 91, 3988–3989.